Polymer-assisted synthesis of $BaTiO_3$ nanorods

J. H. WEI, J. SHI*, Z. Y. LIU
Department of Physics, Wuhan University, Wuhan 430072, People's Republic of China; International Center for Materials Physics, CAS, Shenyang 110016, P.R. China
E-mail: jshi@whu.edu.cn

J. B. WANG
Center for Electron Microscopy, Wuhan University, Wuhan, Hubei 430072, People's Republic China

Recently, quasi one-dimensional (1D) solid nanostructures (nanowires or nanorods) have attracted considerable interest due to their significance in energy sources and optical-electric applications. Compared with micrometer-diameter whiskers and fibers, these nanostructure materials showed remarkable optical, electrical, magnetic, and mechanical properties [1–4]. Among them, $BaTiO_3$ nanoscale materials have been considered as very important ferroelectric materials with potential applications in photoelectric devices, multiplayer ceramic capacitors, auto thermostat meters, etc. [5, 6]. To date, although methods have been developed to synthesize $BaTiO_3$ nanoparticles, little has been reported on the preparation of $BaTiO_3$ nanorods.

The coating technique is widely used to modify the performance of materials. By this technique, Polyaniline (PAn)-$BaTiO_3$ nanocomposites are prepared, with PAn as the core and $BaTiO_3$ as the shell. At the heat-treated process of PAn-$BaTiO_3$ nanocomposite, not only $BaTiO_3$ nanoparticles, but also $BaTiO_3$ nanorods are produced in the final product simultaneously. With the exception of the $BaTiO_3$ nanoparticles, more investigations were performed to identify the formation of $BaTiO_3$ nanorods.

In the experiment, polyaniline was prepared by chemical oxidation of aniline with ammonium peroxydisulfate according to [5]. Precursor solutions for $BaTiO_3$ shell layers were prepared by a sol-gel method. The coatings were processed through the existence of PAn particles by the dip-coating method. The details of the synthesizing process using the sol-gel method can be found in our earlier work [6]. In the experiment, the concentration of the alkoxide in ethanol was 0.5 M; the molar ratio of water, barium ion and diethanolamine to the alkoxide were 1, 1 and 2, respectively. The $BaTiO_3$ gel-coated PAn particles were filtered and dried at 100 °C for 24 h in a vacuum oven and then treated at 1000 °C for 4 h and slowly cooled down to room temperature. The prepared products were collected and kept in a cabinet dryer.

The crystal phase and surface chemistry of the prepared products were analyzed by X-ray powder diffraction (XRD), employing a scanning rate of 0.02°/s in a 2θ range from 10 to 60° (Model Japan Rigaku D/max-γA K_{II}, Cu-target, $\lambda = 0.1541$ nm) and X-ray photoelectron spectrometer (XPS) (Model KRATOS XSAM800, Mg-target). The binding energies obtained in the XPS analysis were standardized for specimens charging using C1s as the reference at 284.6 eV. The morphologies, dimensions, and microstructural characterizations were observed by transmission electron microscopy (TEM, JEM JEOL-2010) and high-resolution transmission electron microscopy (HRTEM, JEOL-2010 FEF), respectively. The formation mechanisms were analyzed by means of the thermogravimetric(TG) and direct pyrolysis chemical ionization mass spectrometry (DPMS), with analysis results deriving from the pure PAn.

Fig. 1 shows the X-ray diffraction pattern of our products, with diffraction peaks similar to those of $BaTiO_3$ bulk crystal. Thus, its diffraction peaks can be indexed as the cubic perovskite structure. $BaTiO_3$ and diffraction data

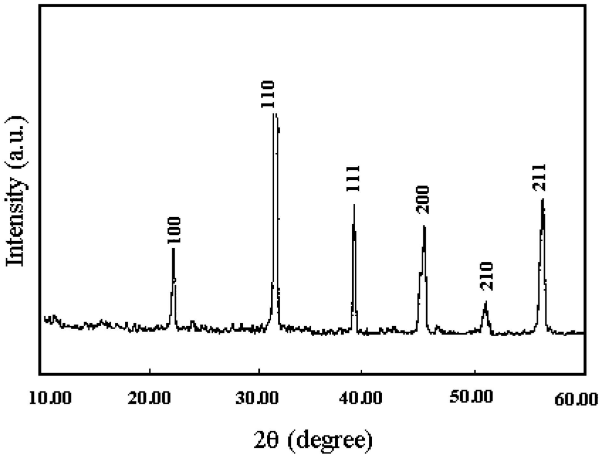

Figure 1 A typical XRD pattern of the as-synthesized products.

---

* Author to whom all correspondence should be addressed.

0022-2461
DOI: 10.1007/s10853-006-5228-5

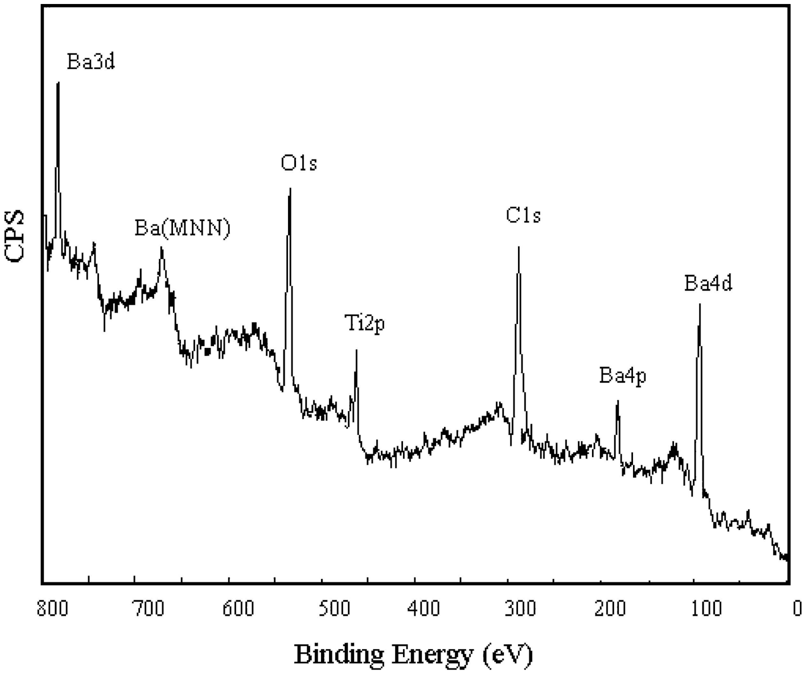

Figure 2 XPS analysis of the as-synthesized products.

were compatible with the JCPDS card of No. 5-626, without any impurities, indicating that the as-prepared product is single phase $BaTiO_3$. Fig. 2 exhibits the XPS pattern of the prepared products, where the peaks at 530.1, 457.9 and 778.6 eV correspond to the binding energy of O1s, Ti2p, and Ba3d, respectively. No other impurity peaks were observed. XRD and XPS analyses identified a high purity of $BaTiO_3$ crystal within the limits of instrumental error.

Furthermore, Fig. 3a, a typical TEM photograph of $BaTiO_3$ nanorods, shows that the diameter and the length of $BaTiO_3$ nanorods are approximately 20–40 nm and 200 nm-5 μm respectively. Fig. 4a is an HRTEM image of a $BaTiO_3$ nanorod with transverse diameter of about 40 ± 0.2 nm. Its lattice fringe image is showed in Fig. 4b, clearly revealing that only the fringes of (2 0 0) planes with a interplanar spacing of about 0.198 nm can be found, indicating that the single $BaTiO_3$ nanorod is single crystalline in nature. Single crystal growth can be ascertained by several ways: The most common way is by introduction of a seed crystal. The other method of single crystal growth may be obtained by starting the crystallization either from a capillary, a pointed vessel, or a ball-shaped tip which is constricted to a narrow neck before widening to the full diameter [7, 8].

Without the presence of PAn in the original particle, the other conditions were the same as described above, the final $BaTiO_3$ grains were planar polygon or near spherical with a diameter of about 25 nm as revealed by Fig. 3b. We suggest that the PAn, a core material in the experiment, must have played an important role to determining the formation of nanorods.

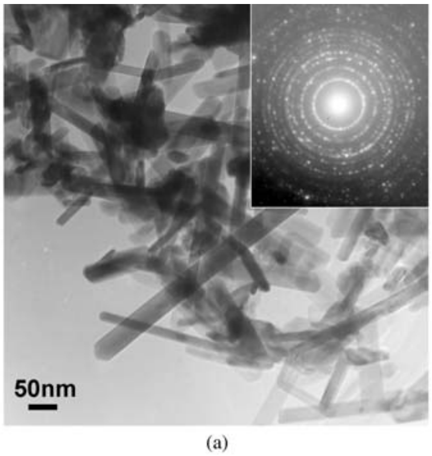

(a)

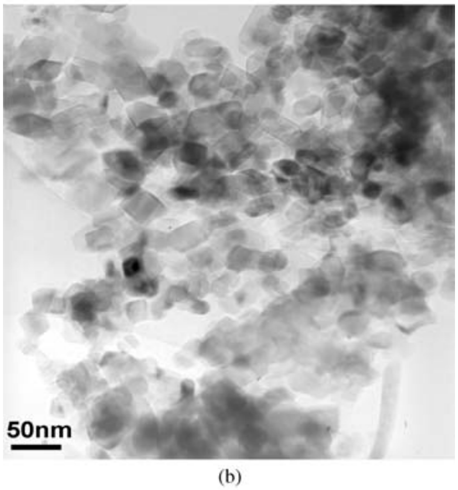

(b)

Figure 3 The TEM image of (a) $BaTiO_3$ nanorods, the inset picture is the electron diffraction pattern from $BaTiO_3$ nanorods and (b) $BaTiO_3$ nanoparticles.

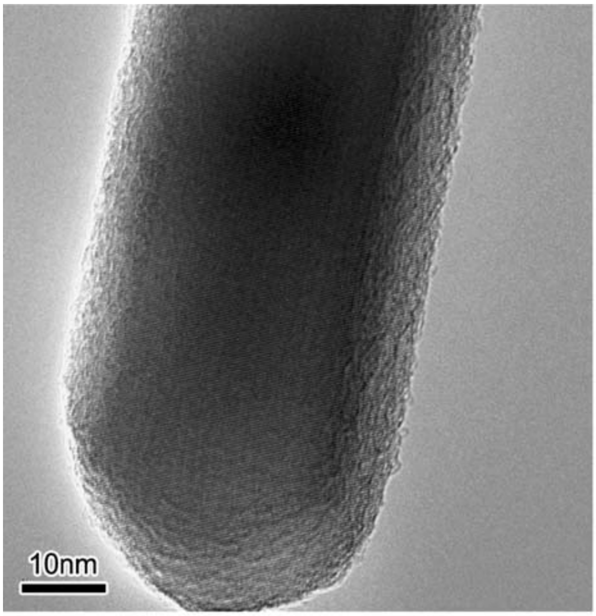

(a) at rather low magnification

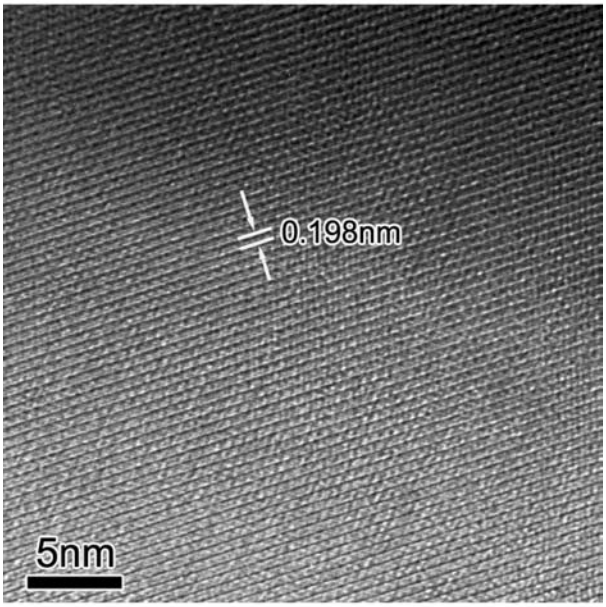

(b) at rather high magnification

Figure 4 The HRTEM images of $BaTiO_3$ nanorod. (a) at rather low magnification. (b) at rather high magnification.

Pradhan *et al*. once pointed out [9, 10] that a reducing environment may enhance the 1D nanostructure growth. From the TG and DPMS analysis results coming from pure PAn [11–14], we know that the degradation process of PAn consists of two or three steps which are attributed to the evolution of water loss of dopants and eventual breakdown of the polymer backbone at about 600 °C. During the process of the polymer backbone breakdown, the $BaTiO_3$ crystallizes and the PAn undergoes a radical decomposition and finally pyrolyzes into linear oligomers of aniline (An). The linear oligomers of An are apt to be volatile and form a reducing environment. The coated particles may take the following reactions:

$$\begin{aligned}&\mathrm{PAn}-\mathrm{BaTiO_3(powders)}\\&\quad\rightarrow n(\mathrm{An}-\mathrm{An})(\mathrm{vapor})+\mathrm{BaTiO_3(solids)}\end{aligned}\qquad(1)$$

From the above reaction, we speculate that $BaTiO_3$ nanorods growth may be attributed to the reducing environment coming from the pyrolysis of PAn-$BaTiO_3$ particles. The detailed formation process may be as follows: Firstly, $BaTiO_3$ particles begin to crystallize at 400 °C and crystallize completely at about 900 °C [15, 16]. At 1000 °C, the size of the $BaTiO_3$ crystal is about 25 nm (Fig. 3b). Secondly, $BaTiO_3$ particles grow along one direction and gradually form nanorods due to the reducing environment coming from reaction (1). The yield of $BaTiO_3$ nanorods gradually increases with time. Finally, the growth of $BaTiO_3$ nanorods gradually stops as the temperature decreases. Concentrations of reduced gases gradually decrease due to the following reaction:

$$n(\mathrm{An}-\mathrm{An})(\mathrm{vapor})\overset{184\,^{\circ}\mathrm{C}}{\Leftrightarrow}n(\mathrm{An}-\mathrm{An})(\mathrm{liquid})\qquad(2)$$

In conclusion, stable core-shell particles consisting of a polyaniline core and a barium titanate shell can form nanorods at suitable temperature conditions. The diameter and the length of the $BaTiO_3$ nanorods are 20–40 nm and 200 nm–5 μm, respectively in the experiment; the formation of $BaTiO_3$ nanorods is most likely controlled by the reducing environment coming from the pyrolysis of PAn-$BaTiO_3$ particles.

Acknowledgments

This work is supported by the National Natural Science Foundation of China (Nos. 10418014 and 10474074), the Open Foundation from State Key Lab of Advanced Technology for Materials Synthesis and Processing of Wuhan University of Technology.

References

1. Y. DAI, Y. ZHANG, Q. K. LI and C. W. NAN, *Chem. Phys. Lett.* **358** (2002) 83.
2. S. J. LIMMER, T. L. HUBLER and G. Z. CAO, *J. sol-gel Sci. Tech.* **26** (2003) 577.
3. C. M. LIU, L. GUO, H. B. XU, Z. Y. WU and J. WEBBER, *Microelectron. Eng.* **66** (2003) 107.
4. N. FERRER-ANGLADA, J. A. GORRI, J. MUSTER, K. LIU, M. BURGHARD and S. ROTH, *Mater. Sci. Eng. C* **15** (2001) 237.
5. J. G. GUAN, "Ph.D. Dissertation" (Huazhong University of Science & Technology, Wuhan, 1995).
6. J. H. WEI, J. G. GUAN and R. Z. YUAN, *J. Wuhan Univ. Technol.-Mater.Sci. Ed.* **17** (2002) 30.
7. E. KALDIS, *J. Phys. Chem. Solids* **26** (1965) 701.
8. B. R. PAMPLIN, "Crystal Growth" (Pergarmon Press, Oxford, 1980).
9. S. K. PRADHAN, P. J. REUCROFT, F. Q. YANG and A. DOZIER, *J. Crystal Growth* **256** (2003) 83.

10. J. W. WANG, Z. X. DENG and Y. D. LI, *Mater. Res. Bull.* **37** (2002) 495.
11. J. H. WEI ‘‘Ph.D. Dissertation” (Wuhan University of Technology, Wuhan, 2002) (in Chinese).
12. C. K. XU, G. D. XU, Y. K. LIU and G. H. WANG, *Solid State Commun.* **122** (2000) 175–179.
13. Y. H. GAO, Y. BANDO, K. KURASHIMA and T. SATO, *J. Mater. Sci.* **37** (2002) 2003–2009.
14. W. D. KINGERY, H. K. BOWEN and D. R. UHLMANN, ‘‘Introduction to ceramics, A Wiley-Interscience Publication” (Wiley &Sons, New York, London, Sydney, Toronto, 1976).
15. J. YU, J. CHU and M. ZHANG, *Appl. Phys. A* **74** (2002) 645.
16. E. CIFTCI, M. N. RAHAMAN and M. SHUMSKY, *J. Mater. Sci.* **36** (2001) 4875.

Received 25 October 2004
and accepted 1 September 2005